SPACE SCIENCES

KAGUYA observation of global emissions of indigenous carbon ions from the Moon

Shoichiro Yokota[1]*, Kentaro Terada[1], Yoshifumi Saito[2], Daiba Kato[3], Kazushi Asamura[2], Masaki N. Nishino[2], Hisayoshi Shimizu[4], Futoshi Takahashi[5], Hidetoshi Shibuya[6], Masaki Matsushima[7], Hideo Tsunakawa[2]

Carbon is a volatile element that has a considerable influence on the formation and evolution of planetary bodies, although it was previously believed to be depleted in the Moon. We present observations by the lunar orbiter KAGUYA of carbon ions emitted from the Moon. These emissions were distributed over almost the total lunar surface, but amounts were differed with respect to lunar geographical areas. The estimated emission fluxes to space were ~5.0×10^4 per square centimeter per second, which is greater than possible ongoing supplies from the solar wind and micrometeoroids. Our estimates demonstrate that indigenous carbon exists over the entire Moon, supporting the hypothesis of a carbon-containing Moon, where the carbon was embedded at its formation and/or was transported billions of years ago.

INTRODUCTION

For decades, it has been believed that carbon and other volatile elements are depleted in the Moon because of early analyses of the Apollo samples (*1*). The notion of a volatile-depleted Moon is one of the greatest premises behind the hypothesis that a giant impact occurred between nascent Earth and Mars-sized body, which generated high-temperature events (*2*). However, the consensus of such a "dry" Moon has subsequently been challenged by advanced analyses that have determined volatile elements, such as water and carbon, in volcanic lunar glasses (*3*, *4*). Analyses of hydrogen isotope and carbon in the deep portions of the lunar materials were used to investigate their origin, respectively. Since the results of these analyses imply that the lunar magma ocean and internal materials contained volatile elements, models based on a giant-impact hypothesis have recently been modified to explain their existence (*5*).

Analyses of meteorites and returned samples are the most precise methods currently available for determining the chemical composition of the parent bodies and investigating their geologic origins and histories, although it is acknowledged that a small number of samples are potentially biased (*6*). The existence of indigenous water in lunar materials has been supported not only by analyses of Apollo samples (*3*) but also by conducting wide-area observations using neutron spectrometers (*7*) and neutral mass spectrometers (*8*) on lunar orbiters. In the case of carbon, however, no such observations have been conducted around the Moon to date (*9*) because both the neutron interactive properties and brightness in the ultraviolet (UV) range are insufficient for spaceborne instruments. It should be noted that neutral mass spectrometers require large abundances of gases emitted from targeted bodies to discriminate them from instrument outgassing, because collected gases are ionized before analyses (*10*).

Emissions of secondary particles, which are caused by interactions with the solar wind, solar UV, and micrometeoroids, are common characteristics of airless small bodies, such as asteroids and moons. Neutral atoms or molecules emitted from the lunar surface form very thin atmosphere (exosphere) (*11*), while a small fraction of the emitted particles are ions. In addition, optical observations by spacecraft have found the lunar exosphere of alkali and noble gas atoms (*9*) and methane molecules (*12*). Although the densities of carbon atoms around the Moon are smaller than the instrumental sensitivities (*9*), it is estimated that secondary ion fluxes sputtered by solar wind bombardments are sufficiently large to be detected by standard spaceborne ion instruments (*13*, *14*). Some of the exospheric particles are ionized mainly by solar UV. Since the emitted ions and photoionized exospheric particles are picked up by the electric and magnetic fields of the solar wind, orbiters can effectively collect these pickup ions when the solar wind conditions are adequate (see Fig. 1) (*15*, *16*). It is considered that these pickup ions may retain information regarding the chemical composition of the surface materials in a similar way to laboratory secondary ion mass spectrometry (SIMS) (*13*, *14*).

In situ observations of lunar ions, which were recently conducted by an ion mass spectrometer on the KAGUYA spacecraft, found C^+ fluxes from the lunar surface (*15*, *17*). In this study, we assess the global existence of indigenous carbon in the Moon using a map of its C^+ emissions derived from 1.5-year KAGUYA observation data.

RESULTS

KAGUYA was a lunar polar orbiter conducting global-mapping observations of the entire surface of the Moon. The nadir-pointing ion mass analyzer (IMA) primarily observed ions originating from the Moon (pickup ions), while the ion energy analyzer (IEA) on the opposite side measured solar wind ions (Fig. 1A) (*17*). In this study, in addition to the ion energy and mass spectrum data from the IMA, we use the magnetic field data (**B**) measured by the lunar magnetometer (LMAG) (*18*) and calculate the electric field (**E**) by $\mathbf{E} = -\mathbf{V} \times \mathbf{B}$, where **V** is the solar wind velocity measured by the IEA (for details, see Materials and Methods).

[1]Graduate School of Science, Osaka University, Machikaneyama-cho, Toyonaka, Japan. [2]Institute of Space and Astronautical Science, Japan Aerospace Exploration Agency, Yoshinodai, Chuo-ku, Sagamihara, Japan. [3]Hitachi Ltd., Research and Development Group, Higashi-Koigakubo, Kokubunji-shi, Tokyo, Japan. [4]Earthquake Research Institute, The University of Tokyo, Yayoi, Bunkyo-ku, Tokyo, Japan. [5]Department of Earth and Planetary Sciences, Faculty of Science, Kyushu University, Motooka, Nishi-ku, Fukuoka, Japan. [6]Department of Earth and Environmental Sciences, Kumamoto University, Kurokami, Kumamoto, Japan. [7]Department of Earth and Planetary Sciences, Tokyo Institute of Technology, Ookayama, Meguro-ku, Tokyo, Japan.
*Corresponding author. Email: yokota@ess.sci.osaka-u.ac.jp

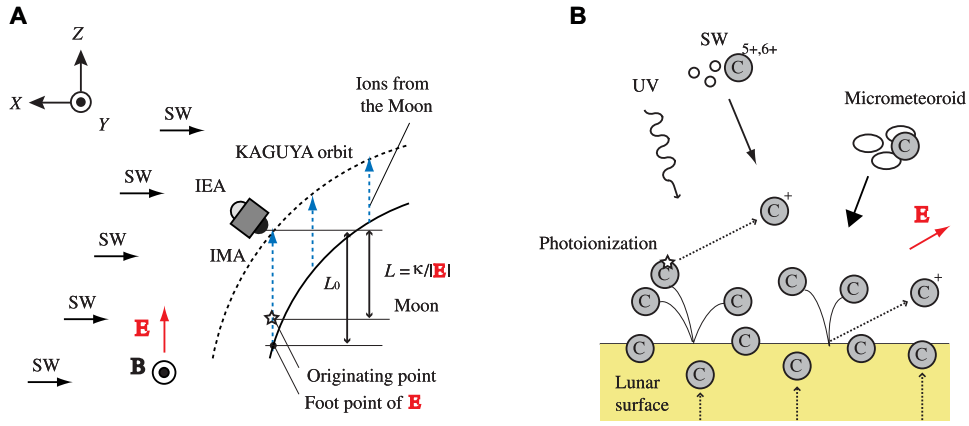

Fig. 1. Pickup ion observation by KAGUYA above the Moon. (**A**) Schematic view of the observation in the Selenocentric Solar Ecliptic coordinates. The solar wind (SW) blows around to the –*x* direction. Two ion sensors, IEA and IMA, on the three-axis stabilized KAGUYA measure mainly solar wind ions and ions emitted from the lunar surface and exosphere, respectively. The solar wind electric and magnetic fields (**E** and **B**) transport (pickup) ions emitted from the Moon. The length, *L*, between the points of origin of measured pickup ions and spacecraft's positions is determined by $L = \kappa/|\mathbf{E}|$, where κ indicates the measured ion energies. Blue arrows denote fluxes of pickup ions. (**B**) Schematic of C^+ emissions due to the solar wind, solar UV, and micrometeoroids. Secondary C^+ emitted from the surface and photoionized exospheric C^+ are picked up by the solar wind to space. The solar wind and micrometeoroids supply carbon to the lunar surface. Indigenous carbon contained in the lunar surface and interior materials contribute substantially to C^+ emissions.

The initial energies of the secondary particles emitted from the surface are less than a few electron volts (*19*). Since the Larmor radius of the ions is much larger than the KAGUYA altitude of 100 km, the pickup ions move in a nearly straight direction along **E** from their points of origin to the spacecraft's position at an altitude of 100 km (*20*). The measured ion energies (κ) are, thus, mainly determined by the acceleration due to **E**, which is expressed by $\kappa \sim |\mathbf{E}|L$, where *L* is the length between the spacecraft's positions and the points of origin of the pickup ions (Fig. 1A). When **E** directs from the lunar surface to the spacecraft, the maximum energy of the ions from the Moon is given by the potential gaps ($\kappa \leq |\mathbf{E}|L_0$) where L_0 denotes the length between the spacecraft's positions and the foot points of **E**. Under ordinary solar wind conditions, the typical values of $|\mathbf{E}|L_0$ is ~200 eV, which is different from the energy of the solar wind H^+ of around 1 keV.

Figure 2 shows an example of ion observations conducted by KAGUYA. The IMA observed intense solar wind protons (H^+) of ~800 eV, which resulted in ghost counts over the entire time-of-flight (TOF)/mass range. In addition, substantial amounts of pickup ions were distributed in the low-energy and wide TOF/mass ranges (Fig. 2A). We derived the TOF/mass spectrum of the lunar pickup ions (Fig. 2B) from ions with energies that were lower than 60% of those of the solar wind H^+. The IMA distinguishes light species (such as He^+, C^+, and O^+) and alkali species from each other, whereas the mass resolution is $M/\Delta M \sim 20$ (*21*).

Using the 1.5-year C^+ data within the full width at half maximum (FWHM) of the calibration curves (Fig. 2B), we built a distribution map of lunar C^+ emissions (Fig. 3). Each foot point of **E** at the lunar surface was used as each point of origin. To reduce contamination from random noise, we selected the data obtained when foot points of **E** were on the dayside lunar surface (for details, see Materials and Methods). To evaluate the background noise level, we rebuilt a figure of IMA ion observations for the same day as those of the observations shown in Fig. 2 but used only data obtained in the lunar wake region (fig. S1), where solar UV and the solar wind are shielded by the Moon. KAGUYA was in the wake around 40% of its revolution. Although KAGUYA detected a small number of solar wind and lunar pickup ions that intruded into the wake, we confirm that the background level was small compared to the signals of the lunar pickup ions shown in Fig. 2.

Figure 3 shows C^+ emissions of ~5.0×10^4 cm^{-2} s^{-1} over large areas above the Moon, which are partly dependent on geographical regions such as the mares and highlands. To verify that the measured C^+ was not related to artificial events such as instrument outgassing (*10*), we compared the energies of measured pickup ions and potential gaps (κ and $|\mathbf{E}|L_0$), both of which were derived from KAGUYA data. The comparison consistently showed that $\kappa \leq |\mathbf{E}|L_0$ (fig. S2), which indicates that the C^+ data were mostly composed of pickup ions generated above or at the lunar surface before being accelerated by **E**. We also compared the distribution map of C^+ emissions (Fig. 3) with the map of the lunar magnetic anomalies observed by the LMAG (fig. S3) (*22*). Since **B** of 10 nT limits the Larmor radius to less than 50 km for 10-eV C^+, some large-scale magnetic anomalies, such as those at the South Pole–Aitken basin, effectively trap ions emitted from the lunar surface. The comparison of the two maps shows that large structures with strong magnetic anomalies agree with the areas of weak C^+ emissions. In addition, we compared each 5° × 5° map pixel (fig. S4). It is shown that large **B** value, derived from lunar magnetic anomalies, effectively limits emissions of C^+. These agreements also suggest that the origin of the measured C^+ was the lunar surface or exosphere. In the remainder of this paper, we consider the lunar magnetic anomalies to discuss the global distribution of C^+ emissions.

DISCUSSION

Although C^+ fluxes of approximately 5.0×10^4 cm^{-2} s^{-1} are distributed over wide areas, the UV spectrometer on Apollo 17 was unable to detect the carbon exosphere. It, thus, provided an estimated upper limit of ~200 atoms cm^{-3} (*23*). The recent far-UV spectrograph on Lunar Reconnaissance Orbiter (LRO) determined a smaller upper carbon density limit of 1.6 atoms cm^{-3} (*9*). In addition, the ionization lifetime of carbon at 1 astronomical unit was observationally

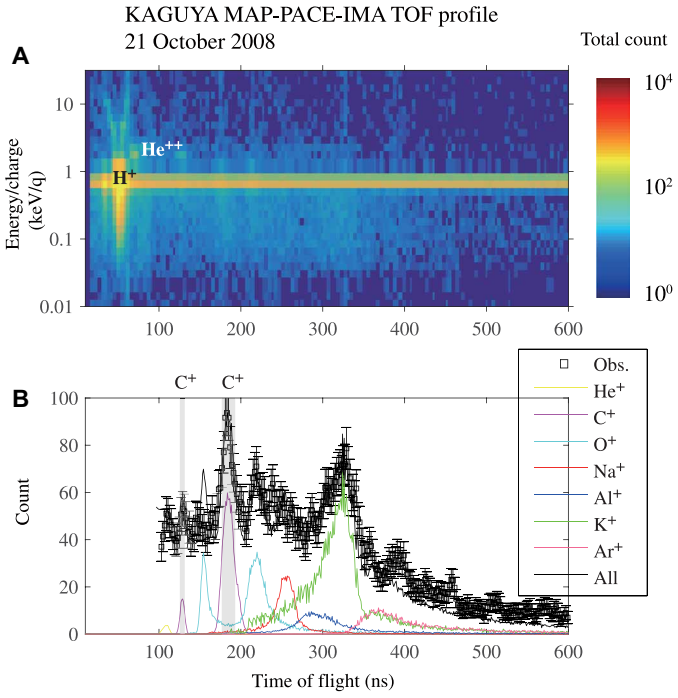

Fig. 2. Observation data by IMA on KAGUYA on 21 October 2008. (**A**) Energy TOF/mass profile of ions. PACE, Plasma energy Angle and Composition Experiment. (**B**) TOF/mass profile of low-energy (<~500 eV) ions derived from data in (A). The black curve is the sum of all calibration curves (colored lines) with random noise to fit the observation data (rectangles). The error bars indicate a confidence interval of 68% (1σ). Three TOF peaks are generated by one sort of incident ions, since ultrathin foil was used for start signals, which resulted in their charge state being converted to negative, neutral, or positive particles in the TOF chamber (*21*). For the incident C^+, the peaks at 140 and 200 ns were made by C^- and a combination of C and C^+, respectively.

estimated at ~10^6 s (*24*). Assuming that the space below KAGUYA at an altitude of 100 km is filled with carbon exosphere of 1.6 atoms cm^{-3}, the exosphere would generate C^+ emissions of 1.6 × 10 ions cm^{-2} s^{-1}. These optical observations, thus, imply that the ionized exospheric particles contribute negligibly to the observed C^+ emissions. The LRO estimated the upper limit of the C^+ density as 0.63 ions cm^{-3} (*7*), which would generate larger C^+ fluxes than the observed C^+ emissions, assuming that C^+ of 0.63 ions cm^{-3} was evenly distributed below the 100-km altitude. Therefore, the C^+ emissions observed by KAGUYA are consistent with previous estimates of the lunar carbon exosphere from optical observations.

If the solar wind and/or micrometeoroid bombardment dominantly cause secondary particle emissions, then the measured pickup ions would partly reflect the surface abundance in a similar way to laboratory SIMS analyses (*13*, *14*). However, the measured C^+ fluxes are of nearly the same order as those of He^+, O^+, and other heavier metallic ions (Fig. 2). Since sample analyses show that the carbon abundance is much smaller than oxygen and metal species (*4*), we consider other source mechanisms for the measured C^+ fluxes. The lunar C^+ may be selectively desorbed by solar UV, as are the lunar Na^+ and K^+ emissions (*25*), and/or may be outgassed from the surface layers and possibly the interior (*26*, *27*) together with the noble gases (*28*).

The Lunar Atmosphere and Dust Environment Explorer observations of the lunar CH_4 exosphere estimated that carbon as CH_4 escapes at a rate of 1.5 × 10^{21} to 4.5 × 10^{21} s^{-1} (*12*). This CH_4 escape flux would be comparable with flux of C^+, if the flux was spatially uniform over the cross section of the Moon (πR_m^2 ~ 10^{17} cm^2, where R_m is the lunar radius). The density of the measured CH_4 exosphere was up to 100s molecules cm^{-3}, nearly equal to the upper limit of the carbon exosphere density (*23*). Even if all CH_4 molecules were dissociated, the CH_4 exosphere might generate the C^+ emission up to 10^3 ions cm^{-2} s^{-1} due to the photoionization lifetime of ~10^6 s (*24*). We conclude that the CH_4 exosphere is not the dominant source of the measured C^+ emissions although the escaping CH_4 exosphere and C^+ emissions are comparable outflows of carbon to space.

The solar wind and micrometeoroids not only stimulate C^+ emissions but also supply carbon to the Moon. The solar wind includes C^{5+} and C^{6+} in addition to H^+, He^{++}, O^{6+}, O^{7+}, and O^{8+} (*29*). The abundance ratios of He/O and C/O in the solar wind are 83.2 and 0.672, respectively (*30*). The He^{++} flux in the solar wind of 3.4 × 10^6 ions cm^{-2} s^{-1} averaged over the KAGUYA observation period was derived from the OMNIWeb. Thus, we estimated 2.7 × 10^4 ions cm^{-2} s^{-1} for the average C^{5+} and C^{6+} fluxes in the solar wind. It should be noted that ~20% of incident solar wind H^+ is back scattered from the lunar surface to space (*31*). Therefore, the KAGUYA observations suggest that only a fraction of the C^+ emitted from the Moon originates from the solar wind.

Micrometeoroids may also continuously supply carbon to the Moon because they are relatively rich in volatile elements (*32*). The micrometeoroid flux to the Moon has been estimated at ~1 × 10^{-16} g cm^{-2} s^{-1} (*33*). If the composition of micrometeoroids is derived from meteorite fluxes to Earth, which consists of 79.5% ordinary chondrite and 4.2% carbonaceous chondrite (*34*), then the carbon supply would be 1.5 × 10^4 atoms cm^{-2} s^{-1}. This estimation supposes that the ordinary and carbonaceous chondrites contain carbon of 0.2 weight % (wt %) (*35*) and 3.5 wt % (*36*), respectively. In the biggest scenario, where the micrometeoroid composition is the same as that of carbonaceous chondrite including carbon of 3.5 wt %, micrometeoroids would supply an amount of 1.7 × 10^5 carbon atoms cm^{-2} s^{-1} to the Moon. Although there are no available direct measurements of the flux and composition of micrometeoroids around the Moon, we conclude that the carbon supply from micrometeoroids is less than the measured C^+ emissions.

The representative C^+ emissions from mares and highlands were calculated by averaging the amounts from the two areas (see Materials and Methods and fig. S5). The observed emissions around lunar mares such as Oceanus Procellarum were substantially higher (5.1 × 10^4 ± 5.4% ions cm^{-2} s^{-1}) than those around highlands (4.5 × 10^4 ± 2.4% ions cm^{-2} s^{-1}). It should be noted that the solar wind and micrometeoroids uniformly supply carbon to the upper stream sides of the Moon and that we estimated this to be a total of 4.2 × 10^4 atoms cm^{-2} s^{-1}. These extraneous carbon supplies are less than the ongoing outflow and are inconsistent with regional differences. The possible explanations for regional differences are not extraneous but internal factors, such as the distributions of C_2H_4 and CO_2 stored in remnants of ancient lunar volcanism (*37*) and/or outgassing paths from the interior reservoir (*26*, *27*). Different from the carbon in volcanic lunar glasses (*4*), which is possibly explained by these extraneous supplies in the lunar volcanically active period, the difference in C^+ emissions between the two areas indicate that the materials of younger mares must relatively retain indigenous carbon within the lunar surface and/or interior portions, as shown in Fig. 1B.

Considering the duration of mare magnetism (*37*) and the depth of young sources, our observations of global and persistent C^+ emissions from the lunar surface suggest that the Moon deeply obtained

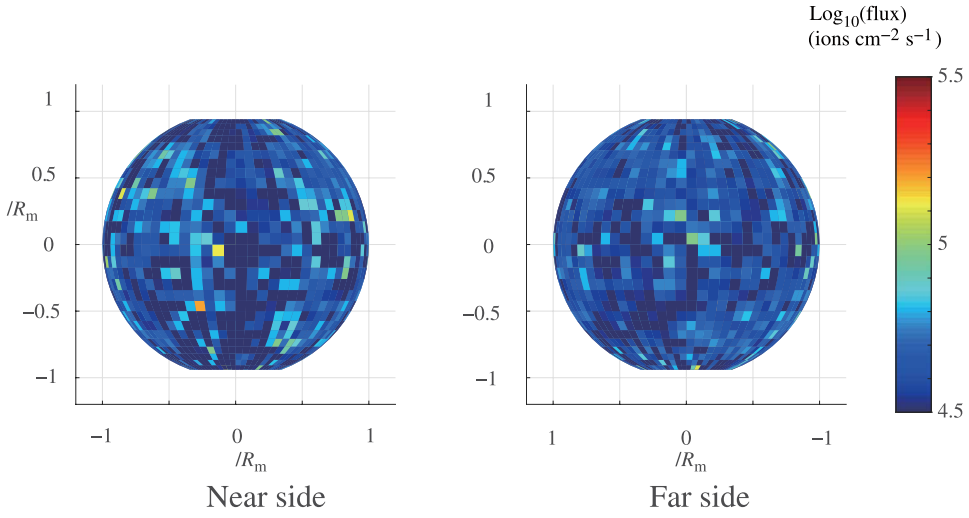

Fig. 3. Orthogonal views of distribution map of C^+ emissions from the Moon. Positions are normalized by the lunar radius (R_m); colors indicate the flux intensity; each pixel size is 5° × 5°. The mean statistical error (1σ) of the C^+ emissions in the pixels is 27%, which is determined with respect to the number of C^+ observations obtained.

nonnegligible carbon at its formation and/or was supplied billion years ago (at least before the lunar cataclysm). Thus, contrary to the notion of a volatile-depleted dry Moon, the observed C^+ emissions unveil a volatile-contained "wet" Moon (*5*). It would be useful to further evaluate initial amounts of volatiles in the Moon, (for example, future isotope analyses of the C^+ emissions from the lunar surface) to provide a quantitative estimation of the mass balance of indigenous carbon, the solar wind, and micrometeoroids.

Last, this study suggests that volatile particles emitted from other small bodies in the solar system could be effectively observed using ion instruments. We, thus, plan to perform secondary ion observations around Mercury and Phobos during the BepiColombo/Mercury Magnetospheric Orbiter and the Martian Moons eXploration missions, respectively.

MATERIALS AND METHODS

Observations by the IMA, IEA, and LMAG onboard the KAGUYA spacecraft

KAGUYA was a lunar polar orbiter that cruised at an altitude of ~30 to 100 km and conducted observations for 1.5 years until it crashed on the lunar surface on 10 June 2009. It contained the scientific instrument known as the MAgnetic field and Plasma experiment (MAP), which comprised the LMAG (*18*, *38*–*40*), IMA, IEA, and two electron sensors (*17*, *41*). The LMAG was a triaxial flux gate magnetometer that measured the magnetic field vector with a sampling frequency of 32 Hz and a resolution of 0.1 nT. The IMA and IEA were capable of measuring three-dimensional distribution functions of ions below 28 keV/q at a resolution of 10% (FWHM) with electrostatic energy analyses and 2π-steradian field of views. The IMA was also equipped with a TOF mass spectrometer at a resolution of $M/\Delta M \sim 20$ (FWHM) (*21*). Since KAGUYA was a three-axis stabilized satellite, the IMA pointed continuously toward the Moon to measure ions mostly coming from the Moon, whereas the IEA was mounted on the opposite side of the spacecraft to measure ions from outer space, such as those in the solar wind (Fig. 1A).

Calculation of C^+ emissions and development of distribution map

Net fluxes of C^+ and solar wind velocities were computed on the ground using calibration data (*42*), obtained during preflight experiments (*21*, *41*) and in-flight specific operations (*17*). Pickup Na^+ fluxes of 4.2×10^4 ions cm^{-2} s^{-1} were estimated around the Moon (*20*) using exospheric sodium densities observed by ground-based telescopes (*43*) and secondary Na^+ yields caused by solar UV (*19*, *25*) and the solar wind (*13*) measured in laboratory experiments. Thus, we used the measured Na^+ fluxes (*44*) to calibrate absolute C^+ fluxes. To build a global distribution map of C^+ emissions, we used C^+ data of which energies were less than 60% of those of the solar wind H^+ and within the FWHM of the C^+ calibration curve in the TOF/mass range (Fig. 2).

Emissions of secondary ions and photoionization require irradiation with the solar wind, solar UV, and/or micrometeoroids. Thus, pickup ion observations above the dayside area are effective. Moreover, the solar wind **E** that transports the ions to the spacecraft is also indispensable (*20*). For the distribution map (Fig. 3), we selected data obtained when KAGUYA was above the dayside surface and when **E** was directed from the Moon to KAGUYA, as shown in Fig. 1A. This data selection was conducted for reducing the background random noise. The foot points of **E** located on the lunar surface were used as the points of origin of measured pickup ions. Under ordinary solar wind conditions, the direction of **B** and **V** are determined within 5° by LMAG (*18*) and IEA (*17*), respectively. Thus, $\mathbf{E} = -\mathbf{V} \times \mathbf{B}$ are calculated at an accuracy of around 7°, which could cause errors of 12 km with respect to the foot point origins of **E**. However, these errors are considered sufficiently small when using the 5° × 5° pixels of the lunar surface except for within the polar regions.

Since the yields and photoionization rates of secondary particles depend on the flux intensities of solar photons and the solar wind, we further selected data obtained when the Moon was outside the terrestrial magnetosphere and sheath region. It should be noted that during the 1.5-year observation period from January 2008 to June 2009, the solar Lyman alpha flux was nearly constant (~3.5 ×

10^{11} photons cm^{-2} s^{-1}) according to the Laboratory for the Atmospheric and Space Physics Interactive Solar Irradiation Data Center and that the solar wind fluxes derived from the OMNIWeb were also stable (~$1.4 \times 10^8 \pm 20\%$ ions cm^{-2} s^{-1}), except for several-time enhancements due to corotating interaction regions, which were excluded. Statistical errors correspond to the SD (1σ).

Estimation of C^+ emissions from mares and highlands

Two representative C^+ emissions from mares and highlands were derived from the global distribution map shown in Fig. 3. We selected the areas at 12.5° to 47.5° north latitude and 22.5° to 77.5° west longitude for the mare and the far side areas at 27.5° to 57.5° north latitude for the highland areas (fig. S5). Since the magnetic anomalies may trap ions emitted from the lunar surface, we selected two areas to avoid the pixels with magnetic fields over 5 nT averaged across the 5° × 5° pixel. The mean C^+ emissions from the selected mare and highland areas were $5.1 \times 10^4 \pm 5.4\%$ ions cm^{-2} s^{-1} and $4.5 \times 10^4 \pm 2.4\%$ ions cm^{-2} s^{-1}, respectively. Statistical errors were determined with respect to the number of C^+ observations obtained (1σ).

SUPPLEMENTARY MATERIALS

Supplementary material for this article is available at http://advances.sciencemag.org/cgi/content/full/6/19/eaba1050/DC1

REFERENCES AND NOTES

1. S. R. Taylor, G. Jeffrey Taylor, L. August Taylor, The moon: A taylor perspective. *Geochim. Cosmochim. Acta* **70**, 5904–5918 (2006).
2. R. M. Canup, E. Asphang, Origin of the Moon in a giant impact near the end of the Earth's formation. *Nature* **412**, 708–712 (2001).
3. A. E. Saal, E. H. Hauri, J. A. Van Orman, M. J. Rutherford, Hydrogen isotopes in lunar volcanic glasses and melt inclusions reveal a carbonaceous chondrite heritage. *Science* **340**, 1317–1320 (2013).
4. D. T. Wetzel, E. H. Hauri, A. E. Saal, M. J. Rutherford, Carbon content and degassing history of the lunar volcanic glasses. *Nat. Geosci.* **8**, 755–758 (2015).
5. M. Nakajima, D. J. Stevenson, Inefficient volatile loss from the Moon-forming disk: Reconciling the giant impact hypothesis and a wet Moon. *Earth Planetary Sci. Lett.* **487**, 117–126 (2018).
6. J. T. Wasson, Sampling the asteroid belt: How biases make it difficult to establish meteorite-asteroid connections. *Meteoritics* **30**, 595 (1995).
7. I. G. Mitrofanov, A. B. Sanin, W. V. Boynton, G. Chin, J. B. Garvin, D. Golovin, L. G. Evans, K. Harshman, A. S. Kozyrev, M. L. Litvak, A. Malakhov, E. Mazarico, T. McClanahan, G. Milikh, M. Mokrousov, G. Nandikotkur, G. A. Neumann, I. Nuzhdin, R. Sagdeev, V. Shevchenko, V. Shvetsov, D. E. Smith, R. Starr, V. I. Tretyakov, J. Trombka, D. Usikov, A. Varenikov, A. Vostrukhin, M. T. Zuber, Mapping of the lunar south pole using the LRO neutron detector experiment LEND. *Science* **330**, 483–486 (2010).
8. M. Benna, D. M. Hurley, T. J. Stubbs, P. R. Mahaffy, R. C. Elphic, Lunar soil hydration constrained by exospheric water liberated by meteoroid impacts. *Nat. Geosci.* **12**, 333–338 (2019).
9. J. C. Cook, S. A. Stern, P. D. Feldman, G. R. Gladstone, K. D. Retherford, C. C. C. Tsang, New upper limits on numerous atmospheric species in the native lunar atmosphere. *Icarus* **225**, 681–687 (2013).
10. P. Wurz, M. Rubin, K. Altwegg, H. Balsiger, J.-J. Berthelier, A. Bieler, U. Calmonte, J. de Keyser, B. Fiethe, S. A. Fuselier, A. Galli, S. Gasc, T. I. Gombosi, A. Jäckel, L. Le Roy, U. A. Mall, H. Rème, V. Tenishev, C.-Y. Tzou, Solar wind sputtering of dust on the surface of 67P/Churyumov-Gerasimenko. *Astron. Astrophys.* **583**, A22 (2015).
11. R. M. Killen, W.-H. Ip, The surface-bounded atmospheres of Mercury and the Moon. *Rev. Geophys.* **37**, 361–406 (1999).
12. R. R. Hodges Jr., Methane in the lunar exosphere: Implications for solar wind carbon excape. *Geophys. Res. Lett.* **43**, 6742–6748 (2016).
13. R. C. Elphic, H. O. Funsten III, B. L. Barraclough, D. J. McComas, M. T. Paffett, D. T. Vaniman, G. Heiken, Lunar surface composition and solar wind-induced secondary ion mass spectrometry. *Geophys. Res. Lett.* **11**, 2165–2168 (1991).
14. M. J. Schaible, C. A. Dukes, A. C. Hutcherson, P. Lee, M. R. Collier, R. E. Johnson, Solar wind sputtering rates of small bodies and ion mass spectrometry detection of secondary ions. *J. Geophy. Res. Planets* **122**, 1968–1983 (2017).
15. S. Yokota, Y. Saito, K. Asamura, T. Tanaka, M. N. Nishino, H. Tsunakawa, H. Shibuya, M. Matsushima, H. Shimizu, F. Takahashi, M. Fujimoto, T. Mukai, T. Terasawa, First direct detection of ions originating from the Moon by MAP-PACE IMA onboard SELENE (KAGUYA). *Geophys. Res. Lett.* **36**, L11201 (2009).
16. J. S. Halekas, A. R. Poppe, G. T. Delory, M. Sarantos, J. P. McFadden, Using ARTEMIS pickup ion observations to place constraints on the lunar atmosphere. *J. Geophys. Res. Planets* **118**, 81–88 (2013).
17. Y. Saito, S. Yokota, K. Asamura, T. Tanaka, M. N. Nishino, T. Yamamoto, Y. Terakawa, M. Fujimoto, H. Hasegawa, H. Hayakawa, M. Hirahara, M. Hoshino, S. Machida, T. Mukai, T. Nagai, T. Nagatsuma, T. Nakagawa, M. Nakamura, K.-I. Oyama, E. Sagawa, S. Sasaki, K. Seki, I. Shinohara, T. Terasawa, H. Tsunakawa, H. Shibuya, M. Matsushima, H. Shimizu, F. Takahashi, In-flight performance and initial results of plasma energy angle and composition experiment (PACE) on SELENE (Kaguya). *Space Sci. Rev.* **154**, 265–303 (2010).
18. H. Tsunakawa, H. Shibuya, F. Takahashi, H. Shimizu, M. Matsushima, A. Matsuoka, S. Nakazawa, H. Otake, Y. Iijima, Lunar magnetic field observation and initial global mapping of lunar magnetic anomalies by MAP-LMAG onboard SELENE(Kaguya). *Rev.* **154**, 219–251 (2010).
19. T. E. Madey, B. V. Yakshinskiy, V. N. Ageev, R. E. Johnson, Desorption of alkali atoms and ions from oxide surfaces: Relative to the origins of Na and K in atmospheres of Mercury and the Moon. *J. Geophys. Res.* **103**, 5873–5887 (1998).
20. S. Yokota, Y. Saito, Estimation of picked-up lunar ions for future compositional remote SIMS analyses of the lunar surface. *Earth Planets Space* **57**, 281–289 (2005).
21. S. Yokota, Y. Saito, K. Asamura, T. Mukai, Development of an ion energy mass spectrometer for application on board three-axis stabilized spacecraft. *Rev. Sci. Instrum.* **76**, 014501 (2005).
22. H. Tsunakawa, F. Takahashi, H. Shimizu, H. Shibuya, M. Matsushima, Surface vector mapping of magnetic anomalies over the Moon using Kaguya and Lunar Prospector observations. *J. Geophys. Res.* **120**, 1160–1185 (2015).
23. P. D. Feldman, D. Morrison, The Apollo 17 ultraviolet spectrometer: Lunar atmosphere measurements revisited. *Geophys. Res. Lett.* **18**, 2105–2108 (1991).
24. J. P. Morgenthaler, W. M. Harris, M. R. Combi, P. D. Feldman, H. A. Weaver, GalexFUV observations of comet c/2004 q2 (Machholz): The ionization lifetime of carbon. *Astrophys. J.* **726**, 8 (2011).
25. B. V. Yakshinskiy, T. E. Madey, Photon-stimulated desorption as a substantial source of sodium in the lunar atmosphere. *Nature* **400**, 642–644 (1999).
26. S. L. Lawson, W. C. Feldman, D. J. Lawrence, K. R. Moore, R. C. Elphic, R. D. Belian, S. Maurice, Recent outgassing from the lunar surface: The Lunar Prospector alpha particle spectrometer. *J. Geophys. Res.* **110**, E09009 (2005).
27. P. H. Schultz, M. I. Staid, C. M. Pieters, Lunar activity from recent gas release. *Nature* **444**, 184–186 (2006).
28. M. Benna, P. R. Mahaffy, J. S. Halekas, R. C. Elphic, G. T. Delory, Variability of helium, neon, and argon in the lunar exosphere as observed by the LADEE. *Geophys. Res. Lett.* **42**, 3723–3729 (2015).
29. G. Gloeckler, F. M. Ipavich, D. C. Hamilton, B. Wilken, W. Stüdemann, G. Kremser, D. Hovestadt, Solar wind carbon, nitrogen and oxygen abundances measured in the Earth's magnetosheath with AMPTE/CCE. *Geophys. Res. Lett.* **13**, 793–796 (1986).
30. D. B. Reisenfeld, R. C. Wiens, B. L. Barraclough, J. T. Steinberg, M. Neugebauer, J. Raines, T. H. Zurbuchen, Solar wind conditions and composition during the genesis mission as measured by in situ spacecraft. *Space Sci. Rev.* **175**, 125–164 (2013).
31. M. Wieser, S. Barabash, Y. Futaana, M. Holmström, A. Bhardwaj, R. Sridharan, M. B. Dhanya, P. Wurz, A. Schaufelberger, K. Asamura, Extremely high reflection of solar wind protons as neutral hydrogen atoms from regolith in space. *Planet. Space Sci.* **57**, 2132–2134 (2009).
32. S. Messenger, F. J. Stadermann, C. Floss, L. R. Nittler, S. Mukhopadhyay, Isotopic signatures of presolar materials in interplanetary dust. *Space Sci. Rev.* **106**, 155–172 (2003).
33. G. Cremonese, P. Borin, A. Lucchetti, F. Marzari, M. Bruno, Micrometeoroids flux on the Moon. *Astron. Astrophys.* **551**, A27 (2013).
34. M. Zolensky, P. Bland, P. Brown, I. Halliday, Flux of extraterrestrial materials, in *Meteorites and the Early Solar System II*, D. S. Lauretta, H. Y. McSween, Eds. (University of Arizona Press, 2006), pp. 869–888.
35. S. Lodders, Solar system abundances and condensation temperatures of the elements. *Astrophys. J.* **591**, 1220–1247 (2003).
36. J. Makjanic, R. D. Vis, J. W. Hovenier, D. Heymann, Carbon in the matrices of ordinary chondrites. *Meteoritics* **28**, 63–70 (1993).
37. D. H. Needham, D. A. Kring, Lunar volcanism produced a transient atmosphere around the ancient Moon. *Earth Planetary Sci. Lett.* **478**, 175–178 (2017).
38. M. Matsushima, H. Tsunakawa, Y.-I. Iijima, S. Nakazawa, A. Matsuoka, S. Ikegami, T. Ishikawa, H. Shibuya, H. Shimizu, F. Takahashi, Magnetic cleanliness program under control of electromagnetic compatibility for the SELENE (Kaguya) spacecraft. *Space Sci. Rev.* **154**, 253–264 (2010).

39. H. Shimizu, F. Takahashi, N. Horii, A. Matsuoka, M. Matsushima, H. Shibuya, H. Tsunakawa, Ground calibration of the high-sensitivity SELENE lunar magnetometer LMAG. *Earth Planets Space* **60**, 353–363 (2008).
40. F. Takahashi, H. Shimizu, M. Matsushima, H. Shibuya, A. Matsuoka, S. Nakazawa, Y. Iijima, H. Otake, H. Tsunakawa, In-orbit calibration of the lunar magnetometer onboard SELENE (KAGUYA). *Earth Planets Space* **61**, 1269–1274 (2009).
41. Y. Saito, S. Yokota, K. Asamura, T. Tanaka, R. Akiba, M. Fujimoto, H. Hasegawa, H. Hayakawa, M. Hirahara, M. Hoshino, S. Machida, T. Mukai, T. Nagai, T. Nagatsuma, M. Nakamura, K.-I. Oyama, E. Sagawa, S. Sasaki, K. Seki, T. Terasawa, Low-energy charged particle measurement by MAP-PACE onboard SELENE. *Earth Planets Space* **60**, 375–385 (2008).
42. Y. Saito, T. Mukai, The method of calculating absolutely calibrated ion and electron velocity moments. *ISAS Res. Note* **815**, 1–23 (2007).
43. A. E. Potter, T. H. Morgan, Coronagraphic observations of the lunar sodium exosphere near the lunar surface. *J. Geophys. Res.* **103**, 8581–8586 (1998).
44. S. Yokota, T. Tanaka, Y. Saito, K. Asamura, M. N. Nishino, M. Fujimoto, H. Tsunakawa, H. Shibuya, M. Matsushima, H. Shimizu, F. Takahashi, Structure of the ionized lunar sodium and potassium exosphere: Dawn-dusk asymmetry. *J. Geophys. Res. Planets* **119**, 798–809 (2014).

Acknowledgments: We are grateful for efforts of the SELENE team. **Funding:** This work was partly supported by Japan Society for the Promotion of Science (JSPS) KAKENHI Grant (nos. 17H01164 and 26800258). **Author contributions:** S.Y. and K.T. wrote the manuscript. S.Y., Y.S., and K.A. contributed to the development, observation, and data processing of IMA and IEA on the KAGUYA spacecraft. S.Y. and D.K. analyzed the data. M.N.N. contributed to the data processing. F.T., M.M., H.Shib., H.Shim., and H.T. contributed to the development, observation, and data processing of LMAG. **Competing interests:** The authors declare that they have no competing interests. **Data and materials availability:** The KAGUYA data used for this study are publicly available at the SELENE Data Archive/DARTS website (https://darts.isas.jaxa.jp/planet/pdap/selene/index.html.en). The solar Lyman alpha flux data and OMNI data were obtained at LISRD (http://lasp.colorado.edu/lisird/) and at OMNIWeb (http://omniweb.gsfc.nasa.gov), respectively.

Submitted 5 November 2019
Accepted 14 February 2020
Published 6 May 2020
10.1126/sciadv.aba1050

Citation: S. Yokota, K. Terada, Y. Saito, D. Kato, K. Asamura, M. N. Nishino, H. Shimizu, F. Takahashi, H. Shibuya, M. Matsushima, H. Tsunakawa, KAGUYA observation of global emissions of indigenous carbon ions from the Moon. *Sci. Adv.* **6**, eaba1050 (2020).